

Flatness-Based Linear Active Disturbance Rejection Control for Tower Crane

Thi Ly Tong

Faculty of Electrical Engineering
Hanoi University of Industry
Hanoi
Vietnam

Tuan Anh Nguyen

School of Electrical and Electronic
Engineering
Hanoi University of Science and
Technology, Hanoi
Vietnam

Minh Duc Duong

School of Electrical and Electronic
Engineering
Hanoi University of Science and
Technology, Hanoi
Vietnam

Controlling tower cranes presents substantial challenges due to their complexity, nonlinearity, and under-actuated dynamics. This paper introduces a control strategy integrating Linear Active Disturbance Rejection Control (LADRC) with differential flatness theory to achieve precise trolley positioning and effective swing elimination. To simplify the system model, we apply differential flatness theory to define the system output, allowing us to treat uncertainties and external disturbances as a singular total disturbance. The control methodology is grounded in LADRC principles. Additionally, we employ Simulated Annealing-Particle Swarm Optimization (PSO-SA) to fine-tune the controller parameters. The simulation results demonstrate that the proposed control method exhibits robust performance against uncertainties.

Keywords: Tower crane, LADRC, Differential flatness, PSO-SA.

1. INTRODUCTION

As modern industry evolves, cranes have become essential transport equipment across various sectors [1,2]. Despite differences in mechanical structures and applications, all crane types share a common trait: the number of independent actuators is fewer than degrees of freedom (DOF), classifying them as underactuated systems.

Underactuated systems provide notable benefits, including energy efficiency, cost reduction, weight savings, and enhanced flexibility compared to fully actuated systems. However, they present significant challenges due to limited control inputs. Consequently, there has been considerable research interest in crane systems over recent decades, particularly regarding the control issues associated with overhead cranes.

In contrast to overhead cranes, tower cranes experience complex rotational motions that introduce additional inertial and centrifugal forces. Moreover, the intricate nonlinear kinematics of tower cranes enhance state coupling, making control tasks—such as precise positioning and swing elimination—more difficult. Thus, controlling tower cranes is inherently more challenging than controlling overhead cranes.

Numerous efforts have been made to address the control challenges of tower cranes using both feedforward and feedback strategies [3]. In recent years, various modern control techniques have been applied to tower cranes. For instance, robust control with input saturation has been explored for tower crane control [4]. Additionally, chattering-free sliding mode control has been implemented to handle uncertain disturbances [5]. Different variations of sliding mode control have also been investigated, including adaptive sliding mode [6-7], non-singular fast terminal sliding mode [8], and

periodic sliding mode control [9]. In [10], an adaptive tracking control approach has been proposed to adapt parameter uncertainties and external disturbances, while another adaptive output feedback control method has been developed in [11] that does not require velocity signal information, simplifying measurement processes.

Intelligent control techniques have also been used to tower crane systems. Neural networks have been used to approximate uncertain or unknown dynamics [12-14], and reinforcement learning has emerged as an adaptive mechanism for controlling these systems [15-16]. Alongside robust and adaptive control methods, active disturbance rejection control (ADRC) has been researched for tower cranes, focusing on observing and mitigating total disturbances [17-18].

In addition to feedback control, several feedforward control strategies have been applied for tower cranes. One approach involves using smooth command inputs to reduce payload oscillations [19]. Another method combines input shaping with fuzzy logic to control the trolley while minimizing payload vibrations [20]. Furthermore, an adaptive input shaping scheme has been developed specifically for swing control, addressing variations in rope length and payload mass [21]. Additionally, flatness control has been utilized as a feedforward controller to suppress vibrations in elastic structure tower cranes [22-23].

Since tower cranes often operate in environments with numerous external disturbances, feedback control strategies are commonly employed. Nevertheless, the majority of these systems are characterized by their complexity and demand for multiple sensors and significant computational resources, rendering practical implementation challenging. Among these, Active Disturbance Rejection Control (ADRC) stands out as a promising approach due to its simplicity and effective disturbance rejection capabilities. Linear ADRC (LADRC) has been demonstrated to be an effective controller in various applications [24-30]. ADRC has also been utilized to control tower crane systems [17-18]. However, due to the significant nonlinearity inherent in tower crane models, ADRC often needs to

Received: March 2025, Accepted: April 2025

Correspondence to: Dr. Minh Duc Duong, Hanoi University of Science and Technology, School of Electrical and Electronic Engineering, Ha Noi, Vietnam, E-mail: duc.duongminh@hust.edu.vn

doi: 10.5937/fme2502270T

© Faculty of Mechanical Engineering, Belgrade. All rights reserved

FME Transactions (2025) 53, 270-279 270

$$\begin{cases}
\ddot{R}(m_p + m_t) - \dot{\gamma}^2 R(m_p + m_t) - l m_p \cos \theta (2\dot{\theta}\dot{\gamma} + \sin \varphi (\dot{\varphi}^2 + \dot{\theta}^2 + \dot{\gamma}^2)) - l \ddot{\gamma} m_p \sin \theta - l \ddot{\theta} m_p \sin \varphi \sin \theta \\
+ l \ddot{\varphi} m_p \cos \varphi \cos \theta - 2l \dot{\varphi} \dot{\theta} m_p \cos \varphi \sin \theta = u_t \\
\ddot{\gamma} (J + R^2 (m_p + m_t) + l^2 m_p (\cos^2 \theta \sin^2 \varphi + \sin^2 \theta)) + 2l m_p R \cos \theta \sin \varphi - l m_p \ddot{R} \sin \theta + \dot{\gamma} R \dot{R} (2m_p + 2m_t) \\
+ l \ddot{\theta} m_p (l \sin \varphi + R \cos \theta) - l \dot{\theta} m_p R \sin \theta (\dot{\theta} + 2\dot{\gamma} \sin \varphi) + 2l^2 \dot{\theta} \dot{\varphi} m_p \cos \theta \varphi \sin^2 \theta - l^2 \ddot{\varphi} m_p \cos \varphi \cos \theta \sin \theta \\
+ 2l \dot{\gamma} m_p \dot{R} \cos \theta \sin \varphi + l^2 \dot{\varphi} \dot{\gamma} m_p \sin 2\varphi \cos^2 \theta + l^2 \dot{\theta} \dot{\gamma} m_p \sin 2\theta \cos^2 \varphi + 2l \dot{\varphi} \dot{\gamma} m_p R \cos \varphi \cos \theta + l^2 \dot{\varphi}^2 m_p \cos \theta \sin \varphi \sin \theta = u_r \quad (1) \\
l^2 \ddot{\varphi} m_p \cos^2 \theta + l g m_p \cos \theta \sin \varphi - 2l^2 \dot{\theta} m_p \cos \theta (\dot{\varphi} \sin \theta + \dot{\gamma} \cos \varphi \cos \theta) - l^2 \ddot{\gamma} m_p \cos \varphi \cos \theta \sin \theta + l m_p \ddot{R} \cos \varphi \cos \theta \\
- l \dot{\gamma}^2 m_p \cos \varphi \cos \theta (R + l \cos \theta \sin \varphi) = 0 \\
l^2 \ddot{\theta} m_p + l \dot{\gamma} m_p (l \sin \varphi + R \cos \theta) - l m_p \ddot{R} \sin \varphi \sin \theta + 2l \dot{\gamma} m_p \dot{R} \cos \theta + l \dot{\gamma}^2 m_p (R \sin \varphi \sin \theta - l \cos^2 \varphi \cos \theta \sin \theta) \\
+ l g m_p \cos \varphi \sin \theta + l^2 \dot{\theta}^2 m_p \cos \theta \sin \theta + 2l^2 \dot{\varphi} \dot{\gamma} m_p \cos \varphi \cos^2 \theta = 0
\end{cases}$$

2. DYNAMICS OF TOWER CRANES

The tower crane system is shown in Figure 1. This study focuses solely on the translational movement of the trolley, the rotational motion of the tower boom, and the vibrational dynamics of the payload. Notably, variations in rope length and the elastic deformations of the crane are disregarded. The dynamic formulation (1) of the tower crane is derived using the Euler-Lagrange approach, detailed in [34]. The meanings of model parameters are shown in Table 1.

Equation (1) exhibits a character of nonlinearity and complexity. Moreover, the first two equations in (1) describe the relation between system inputs and the motion of the tower crane. The last two equations express the relation between the payload's swing angles and jib-trolley movement, conspicuously devoid of any direct system inputs. Consequently, the system is classified as under-actuated, featuring a mere two inputs yet yielding four outputs. This complexity presents a formidable challenge in designing a controller suitable for a tower crane.

Table 1. List of tower crane model parameters

Symbol	Meaning
m_t	Trolley mass (kg)
m_p	Payload mass (kg)
R	Trolley displacement (m)
γ	Jib slew angle (rad)
φ, θ	Payload swing angle (rad)
l	Length of rope (m)
g	Gravity acceleration (m/s^2)
u_t	Control force of trolley translation (N)
u_r	Control torque of jib slew (N.m)

3. FLAT ATTRIBUTE DETERMINATION

Given the constraint of limited swing angles, where the maximum oscillation angles of the tower crane φ_{\max} and θ_{\max} are constrained to 10° ; the proposed control methodology guarantees adherence to this condition. Under this assumption, the approximation is satisfied: $\sin \alpha \approx \alpha$; $\cos \alpha \approx 1$ with $\alpha = \varphi, \theta$. Consequently, the coordinates of the payload (x, y, z) in the coordinate system OX1Y1Z1 affixed to the tower crane are delineated accordingly by the following equations:

$$\begin{cases}
x = R \cos \gamma + l \varphi \cos \gamma - l \theta \sin \gamma \\
y = R \sin \gamma + l \varphi \sin \gamma + l \theta \cos \gamma \\
z = -l
\end{cases} \quad (2)$$

By introducing an additional system variable, namely the cable tension force T , the motion of the payload can be written according to Newton's second law as:

$$\begin{cases}
m\ddot{x} = -(T \varphi \cos \gamma - T \theta \sin \gamma) \\
m\ddot{y} = -(T \varphi \sin \gamma - T \theta \cos \gamma) \\
m\ddot{z} = T - mg
\end{cases} \quad (3)$$

From (2) and (3), all system variables $(R, \gamma, \varphi, \theta)$ can be parametrized as functions of x, y, \ddot{x}, \ddot{y} , as follows:

$$\begin{cases}
R = \sqrt{\left(x + \frac{l}{g} \ddot{x}\right)^2 + \left(y + \frac{l}{g} \ddot{y}\right)^2} \\
\gamma = \arctan \left(\frac{y + \frac{l}{g} \ddot{y}}{x + \frac{l}{g} \ddot{x}} \right) \\
\varphi = \frac{-\left(x + \frac{l}{g} \ddot{x}\right) \ddot{x} - \left(y + \frac{l}{g} \ddot{y}\right) \ddot{y}}{g \sqrt{\left(x + \frac{l}{g} \ddot{x}\right)^2 + \left(y + \frac{l}{g} \ddot{y}\right)^2}} \\
\theta = \frac{\left(y + \frac{l}{g} \ddot{y}\right) \ddot{x} + \left(x + \frac{l}{g} \ddot{x}\right) \ddot{y}}{g \sqrt{\left(x + \frac{l}{g} \ddot{x}\right)^2 + \left(y + \frac{l}{g} \ddot{y}\right)^2}}
\end{cases} \quad (4)$$

By expressing all state variables in terms of load coordinates (x, y) , it follows that the tower crane system possesses flatness, with load coordinates serving as the flat output. Leveraging this flatness property, the tower crane model can be transformed into a canonical form, facilitating the straightforward design of a simple yet efficient controller for the system.

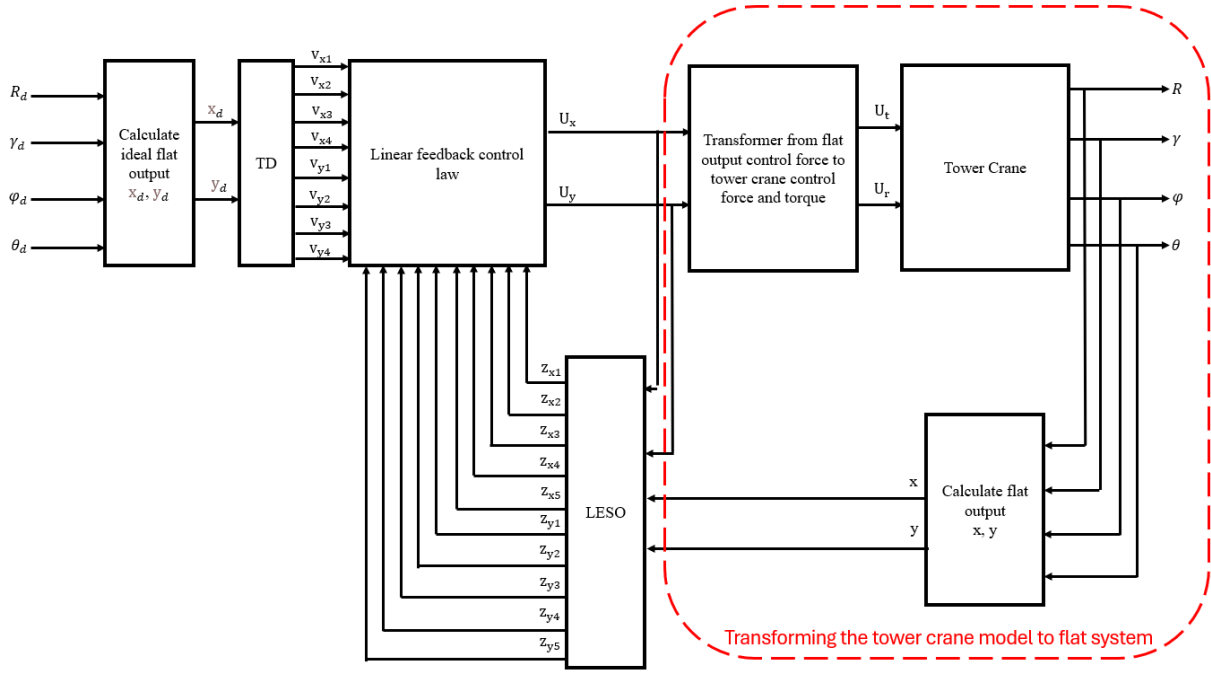


Figure 2. Structural Diagram of ADRC Controller

4. DESIGN OF LARDC METHOD FOR TOWER CRANE

4.1 Controller Structure

As demonstrated earlier, a tower crane is a flat system where the payload coordinates (x, y) serve as the flat output. This characteristic enables the transformation of the tower crane model into canonical form, facilitating the design of a Linear Active Disturbance Rejection Controller (LADRC) tailored for the converted system. The structural diagram depicting the comprehensive system is delineated in Figure 2.

In Figure 2, $R_d, \gamma_d, \phi_d, \theta_d$ symbolize the reference positions for the trolley along the jib, the jib's angular rotation, and the payload's oscillation angles. Correspondingly, R, γ, ϕ, θ represent the actual tower crane model outputs. Likewise, (x_d, y_d) and (x, y) denote the reference flat output and the actual flat output, achievable through computations based on the tower crane's reference and actual positions. The setup integrates a Tracking Differentiator (TD), a core controller, and a Linear Extended State Observer (LESO). The TD softens the flat reference signal and computes the reference state input $v_{ij}(i = x, y; j = 1, 2, 3, 4)$ for the controller. Concurrently, the LESO estimates the model states $z_{ij}(i = x, y; j = 1, 2, 3, 4)$ alongside the total disturbances z_{x5}, z_{y5} inherent in the transformed model. The controller derives the control signal by considering the estimated total disturbances and the differences $(v_{ij} - z_{ij})$ between the reference state inputs and the estimated states.

Set F_x and F_y respectively are the two forces acting on the payload along the x and y axes in a fixed coordinate system $OX_1Y_1Z_1$. The relation between (F_x, F_y) and (U_t, U_r) is expressed in (5):

$$\begin{bmatrix} U_t \\ U_r \end{bmatrix} = J^T \begin{bmatrix} F_x \\ F_y \end{bmatrix} \quad (5)$$

$$\text{with } J^T = \begin{pmatrix} \cos \gamma & \sin \gamma \\ -R \sin \gamma & R \cos \gamma \end{pmatrix}.$$

Set the state variables as $x_1 = x, x_2 = \dot{x}, x_3 = \ddot{x}, x_4 = x^{(3)}, y_1 = y, y_2 = \dot{y}, y_3 = \ddot{y}, y_4 = y^{(3)}$. From equations (1), (4), and (5), the tower crane model is converted to the form as follows:

$$\begin{cases} \dot{x}_1 = x_2 \\ \dot{x}_2 = x_3 \\ \dot{x}_3 = x_4 \\ \dot{x}_4 = f_x(x_2, x_3, x_4, y_2, y_3, y_4) + b_{1x}F_x + b_{2x}F_y \\ \dot{y}_1 = y_2 \\ \dot{y}_2 = y_3 \\ \dot{y}_3 = y_4 \\ \dot{y}_4 = f_y(x_2, x_3, x_4, y_2, y_3, y_4) + b_{1y}F_y + b_{2y}F_x \end{cases} \quad (6)$$

where $b_{1x} = \frac{\partial x_4}{\partial F_x}; b_{2x} = \frac{\partial x_4}{\partial F_y}; b_{1y} = \frac{\partial y_4}{\partial F_x}; b_{2y} = \frac{\partial y_4}{\partial F_y}$. Two

functions f_x and f_y correspond to total disturbances of the system. It is noted that LESO will estimate these two functions, the detailed calculation of them is not necessary.

Next, to decouple the x and y channels, we set

$$\begin{cases} U_x = b_{1x}F_x + b_{2x}F_y \\ U_y = b_{1y}F_y + b_{2y}F_x \end{cases} \quad (7)$$

Then,

$$\begin{cases} F_x = \frac{b_{1y}U_x - b_{2x}U_y}{b_{1x}b_{1y} - b_{2x}b_{2y}} \\ F_y = -\frac{b_{2y}U_x - b_{1x}U_y}{b_{1x}b_{1y} - b_{2x}b_{2y}} \end{cases} \quad (8)$$

And the model (6) becomes:

$$\begin{cases} \dot{x}_1 = x_2 \\ \dot{x}_2 = x_3 \\ \dot{x}_3 = x_4 \\ \dot{x}_4 = f_x(x_2, x_3, x_4, y_2, y_3, y_4) + b_x U_x \\ \dot{y}_1 = y_2 \\ \dot{y}_2 = y_3 \\ \dot{y}_3 = y_4 \\ \dot{y}_4 = f_y(x_2, x_3, x_4, y_2, y_3, y_4) + b_y U_y \end{cases} \quad (9)$$

Choosing $(b_{0x}, b_{0y}) = const$ are the estimated values of b_x, b_y respectively, (9) can be rewritten as (10).

$$\begin{cases} \dot{x}_1 = x_2 \\ \dot{x}_2 = x_3 \\ \dot{x}_3 = x_4 \\ \dot{x}_4 = f_{0x}(x_2, x_3, x_4, y_2, y_3, y_4) + b_{0x} U_x \\ \dot{y}_1 = y_2 \\ \dot{y}_2 = y_3 \\ \dot{y}_3 = y_4 \\ \dot{y}_4 = f_{0y}(x_2, x_3, x_4, y_2, y_3, y_4) + b_{0y} U_y \end{cases} \quad (10)$$

where (s_{0x}, f_{0y}) are the total disturbances,

$$\begin{aligned} f_{0x} &= f_x - (b_x - b_{0x})U_x \\ f_{0y} &= f_y - (b_y - b_{0y})U_y \end{aligned}$$

A LADRC controller will be designed for the system in (10), where the control signal (U_x, U_y) are established from the reference state v_{ij} , estimated states and estimated total disturbances z_{ij} of the system.

4.2 LADRC Controller Design

4.2.1 Design a Tracking Differentiator (TD)

In the context of the tower crane system featuring the flat output (x, y) , the designated reference flat output is denoted by (x_d, y_d, z_d) . According to (2):

$$\begin{cases} x_d = R_d \cos \gamma_d + l\varphi_d \cos \gamma_d - l\theta_d \sin \gamma_d \\ y_d = R_d \sin \gamma_d + l\varphi_d \sin \gamma_d + l\theta_d \cos \gamma_d \end{cases} \quad (11)$$

In (11), x_d and y_d are the reference horizontal and vertical displacement of the payload. Angles φ_d and θ_d are the desired oscillation angles of the system, and they are set to 0 for vibration suppression. Therefore, (11) can be further implied as:

$$\begin{cases} x_d = R_d \cos \gamma_d \\ y_d = R_d \sin \gamma_d \end{cases} \quad (12)$$

The input of the TD can be calculated using (12). The TD is designed as follows:

$$\begin{cases} \dot{v}_{i1} = v_{i2} \\ \dot{v}_{i2} = v_{i3} \\ \dot{v}_{i3} = v_{i4} \\ \dot{v}_{i4} = -r_i(r_i(r_i(r_i(v_{i1} - v_{i0}) + 4v_{i2}) + 6v_{i3}) + 4v_{i4})) \end{cases}, (i = x, y) \quad (13)$$

where,

v_{i0} is the set value corresponding to the x_d, y_d .

v_{i1} is the orbit converted by the TD.

v_{i2} is a derivative of v_{i1} .

v_{i3} is the second derivative of v_{i1} .

v_{i4} is the third derivative of v_{i1} .

r_i is the time constant used to adjust the performance of the TD unit.

4.2.2 Design of a Linear Extended State Observer (LESO)

A Linear Extended State Observer is built as follows:

$$\begin{cases} e_i = z_{i1} - i \\ \dot{z}_{i1} = z_{i2} - \beta_{i1}e_i \\ \dot{z}_{i2} = z_{i3} - \beta_{i2}e_i \\ \dot{z}_{i3} = z_{i4} - \beta_{i3}e_i \\ \dot{z}_{i4} = z_{i5} - \beta_{i4}e_i + b_{0i}U_i \\ \dot{z}_{i5} = -\beta_{i5}e_i \end{cases}, (i = x, y) \quad (14)$$

In which z_{i1}, z_{i2}, z_{i3} and z_{i4} are the estimated values of $i, \dots, 0, i, i, i, i$, and z_{i5} is the estimated value of f_{0i} ($i=x, y$). $\beta_{i1}, \beta_{i2}, \beta_{i3}, \beta_{i4}, \beta_{i5}$ are the coefficients of the observer. To ensure the convergence of the observer, the coefficients must satisfy the following relationship:

$$s^5 + \beta_{i1}s^4 + \beta_{i2}s^3 + \beta_{i3}s^2 + \beta_{i4}s + \beta_{i5} = (s + w_{oi})^5 \quad (15)$$

where w_{oi} lies on the left half-side of the complex plane. Therefore, the coefficients of the observer are calculated as follows:

$$\begin{cases} \beta_{i1} = 5w_{oi} \\ \beta_{i2} = 10w_{oi}^2 \\ \beta_{i3} = 10w_{oi}^3 \\ \beta_{i4} = 5w_{oi}^4 \\ \beta_{i5} = w_{oi}^5 \end{cases} \quad (16)$$

with w_{oi} is the bandwidth of the observer.

4.2.3 State feedback controller design

The control law can be designed as follows:

$$\begin{cases} e_{i1} = v_{i1} - z_{i1} \\ e_{i2} = v_{i2} - z_{i2} \\ e_{i3} = v_{i3} - z_{i3} \\ e_{i4} = v_{i4} - z_{i4} \\ u_{0i} = \alpha_{i1}e_{i1} + \alpha_{i2}e_{i2} + \alpha_{i3}e_{i3} + \alpha_{i4}e_{i4} \\ U_i = \frac{u_{0i} - z_{i5}}{b_{0i}} \end{cases}, (i = x, y) \quad (17)$$

In which $\alpha_{i1}, \alpha_{i2}, \alpha_{i3}$, and α_{i4} are the coefficients of the controller.

To ensure the stability of the system, four closed-loop poles are placed at $-w_{ci}$. Then, the coefficients of the controller must be satisfied:

$$s^4 + \alpha_{i1}s^3 + \alpha_{i2}s^2 + \alpha_{i3}s + \alpha_{i4} = (s + w_{ci})^4 \alpha_{i1} \quad (18)$$

where w_{oi} lies on the left half-side of the complex plane. Therefore, the coefficients of the controller are calculated as follows:

$$\begin{cases} \alpha_{i1} = 4w_{ci} \\ \alpha_{i2} = 6w_{ci}^2 \\ \alpha_{i3} = 4w_{ci}^3 \\ \alpha_{i4} = w_{ci}^4 \end{cases} \quad (19)$$

With w_{ci} is the bandwidth of the controller.

Through fine-tuning w_{oi} and w_{ci} , one can identify the optimal controller and observer tailored for the tower crane system.

4.3 Controller Parameter Optimization

Due to the alignment between w_{oi} and w_{ci} , and the uncertain rules for synchronizing the settings of the ADRC controller, adjusting its parameters is still a significant challenge. By studying intelligent optimization algorithms in the control field, the PSO-SA optimization algorithm is proposed to determine the optimized parameters for ADRC controllers. PSO-SA [33] is an effective global optimization method that can avoid local optimization points.

The optimization problem's goal is to minimize the settling time of the trolley-jib motion and the total deviation of the swing angle during operation while the control input signal is limited. On that basis, the fitness function for the optimal algorithm is chosen as follows:

$$J = T_{xl} + \mu \int_0^{\infty} (|\varphi(t)| + |\theta(t)|) dt \quad (20)$$

In which,

- $T_{xl} = \max(T_{xLR}, T_{xl}\gamma)$ is the maximum of the settling time of the trolley and jib motion;
- $\int_0^{\infty} (|\varphi(t)| + |\theta(t)|) dt$ is the total deviation of the two swing angle values from the beginning to the end.
- μ is the scale parameter between setting time and total deviation of swing angles. In this research, μ is set to be 2.

The control input signals for trolley and jib control are constrained within the threshold limits of U_{tlim} and U_{rlim} , respectively. In this study, for simulation purposes, U_{tlim} and U_{rlim} are predetermined at a value of 10.

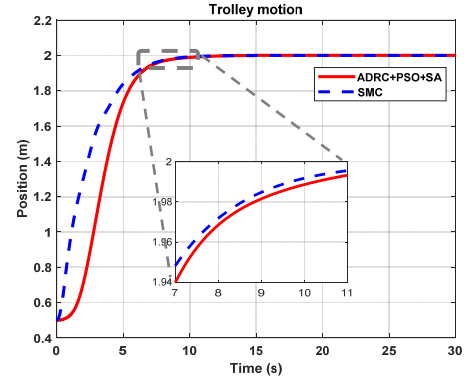
5. SIMULATION RESULTS

Simulation was conducted within the Matlab/Simulink framework to validate the performance of the proposed controller. A comparative analysis was also performed between the proposed controller and the SMC controller. The system model parameters are delineated in Table 1. The simulation scenario is described as follows: Initially, the trolley is positioned at $R_0 = 0.5$ m, and the jib is aligned at an angle of $\gamma = 0^\circ$. The target positions for the trolley and jib are set at $R_d = 2$ m and γ_d

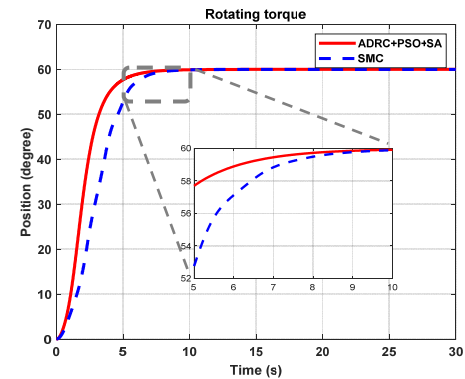
$= 60^\circ$, respectively. The simulation outcomes are depicted in Figure 5.

Table 2. System simulation model parameters

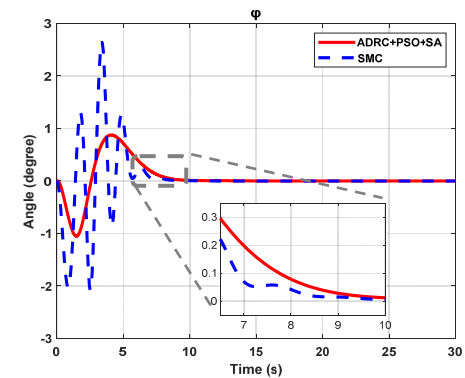
g	l	m_t	m_p	J	W_{0x}
9.81m/s ²	1m	7kg	1kg	6.8kg.m ²	40.765
W_{cx}	W_{0y}	W_{cy}	r_x	r_y	-
1.699	46.131	1.979	1.186	1.186	-



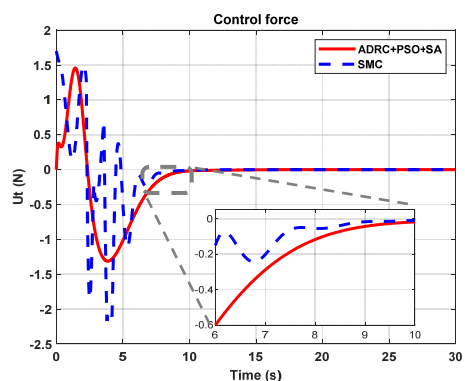
(a) First scenario – trolley motion



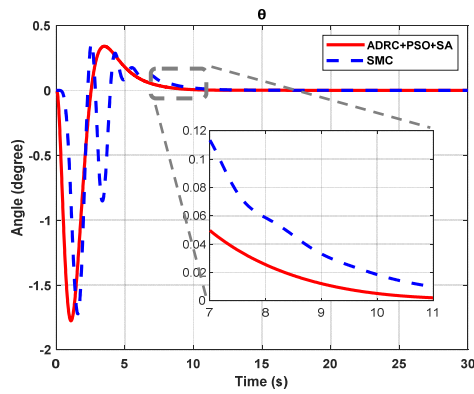
(b) First scenario – jib motion



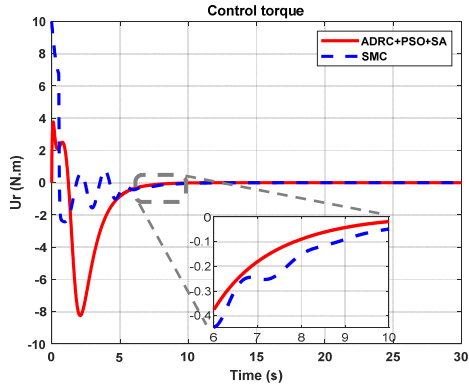
(c) First scenario – swing angle φ



(d) First scenario – swing angle θ



(e) First scenario- trolley control input



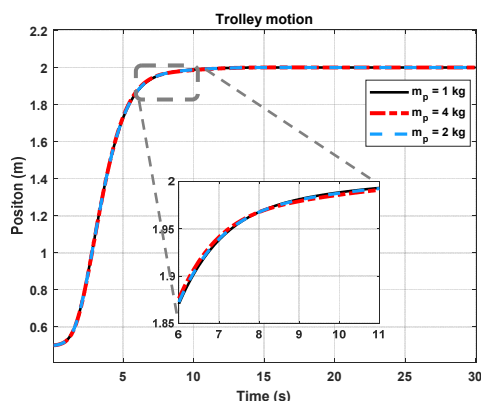
(f) First scenario - jib control input

Figure 5. Simulation results

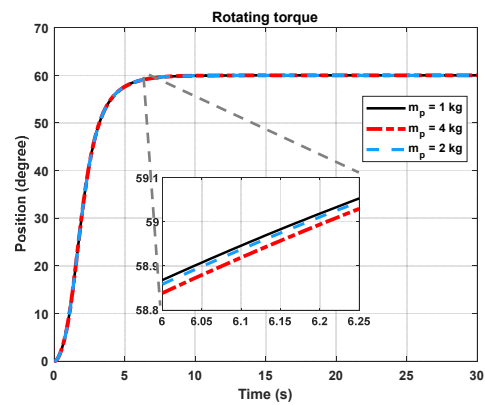
Employing the proposed controller ensures rapid and precise positioning of both the trolley and jib. The trolley's settling time is recorded at 7.65 seconds, while the jib achieves stability in 5.92 seconds. Additionally, the maximum swing angle remains minimal (under 2 degrees), leading to swift suppression of payload vibration. A comparison with the SMC controller was conducted to validate the effectiveness of the proposed controller. The comparative results are presented in Figure 5 and Table 2.

Table 3. Comparison results between the proposed and the SMC controllers

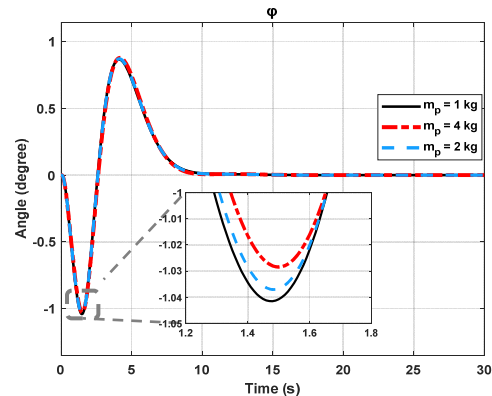
Parameter	SMC	Flatness-ADRC
Trolley settling time	7.15	7.65
Jib settling time	6.18	5.92
φ_{max}	2.65	1.04
θ_{max}	1.71	1.75
U_{tmax} (N)	2.15	1.45
U_{rmax} (Nm)	10	8.2



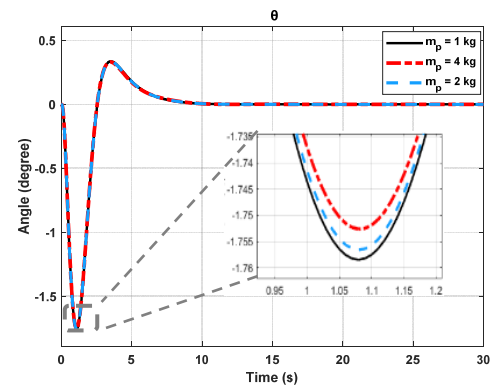
(a) Payload mass change- trolley position



(b) Payload mass change - jib position



(c) Payload mass change - swing angle φ



(d) Payload mass change - swing angle θ

Figure 6. Simulation results of payload mass change

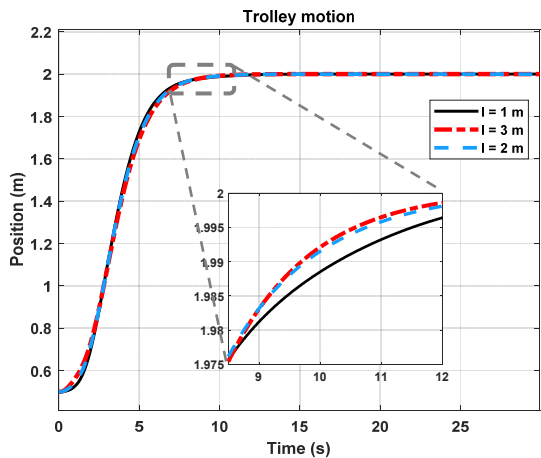
From the comparison results in Table 2, it is observed that the proposed controller's settling time for trolley motion is slightly slower than that of the SMC controller, while the settling time for the jib motion is faster. The difference in settling times is marginal (0.5 seconds for trolley motion and 0.26 seconds for jib motion). However, the maximum oscillation amplitude of the payload oscillation angles is significantly smaller with the proposed controller (φ_{max} of SMC is twice as large as the proposed controller). Notably, the number of payload oscillations with the SMC is greater than with the proposed controller. Thus, the effectiveness of the proposed method is clearly demonstrated.

Furthermore, to demonstrate the robustness of the proposed controller under system uncertainties, the following simulations were conducted:

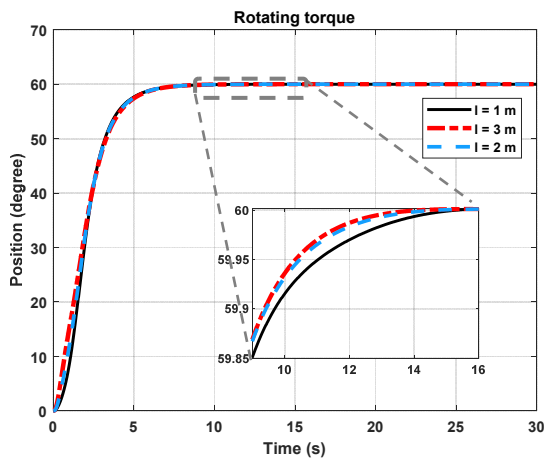
- The payload mass was varied to 2 kg and 4 kg.
- The rope length was adjusted to 2 m and 3 m.

The simulation results are illustrated in Figure 6 for varying payload mass and Figure 7 for changing rope length.

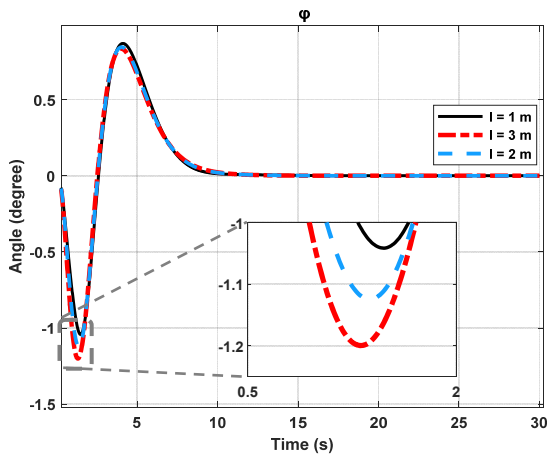
The system remained stable, exhibiting excellent position tracking and effectively suppressed payload vibration despite the variations in payload mass and rope length. As shown in Figure 6, an increase in payload mass slightly prolongs the settling time, while the oscillation amplitude diminishes. In Figure 7, as the rope length increases, the maximum oscillation angle φ_{max} increases, whereas θ_{max} slightly decreases. The settling time for both trolley and jib motions increases marginally. The controller demonstrates strong resilience to disturbances, maintaining performance even with inaccurately assessed payload mass and rope length.



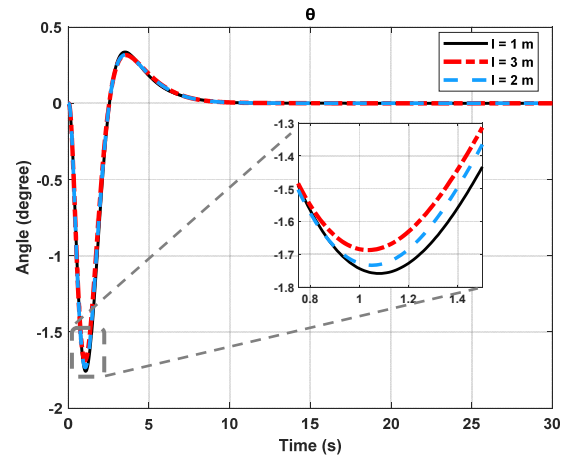
(a) Rope length change- trolley position



(b) Rope length change- jib position



(c) Rope length change- swing angle φ



(d) Rope length change- swing angle θ

Figure 7. Simulation results of rope length change.

6. CONCLUSION

This paper proposes a flatness-based Linear Active Disturbance Rejection Control approach for tower crane systems. The tower crane system is reformulated into a canonical form, thereby enabling the effective implementation of Linear Active Disturbance Rejection Control. The designing process is clearly specified and the control parameters can be determined using Simulated Annealing - Particle Swarm Optimization to minimize swing angles and settling time. Despite the system's inherent lack of an implementation mechanism and the dynamic model's complex nonlinear constraints and coupling among state variables, the proposed flatness-based ADRC controller successfully meets the anti-vibration requirements. The system rapidly reaches a steady state, completely suppressing residual oscillations. Compared to the SMC controller, the proposed controller exhibits superior performance. Additionally, the robustness of the proposed controller against model parameter uncertainties has been validated through simulation.

With a clear and streamlined design process, the proposed methodology can be readily implemented in practical applications utilizing widely adopted industrial controllers, such as Programmable Logic Controllers (PLCs). In the near future, the practical implementation of the proposed controller in a tower crane system will be evaluated. Furthermore, the flexibility of the tower crane structure will be considered.

REFERENCES

- [1] Singhose, W., Lawrence J., Sorensen K., Kim D.: Applications and Educational Uses of Crane Oscillation Control, FME Transactions, Vol. 34, No. 4, pp. 175-183, 2006.
- [2] Sawodny O., Neupert J., Arnold E.: Actual Trends in Cran Automation – Directions for the Future, FME Transactions, Vol. 37, No. 4, pp. 167-174, 2009.
- [3] Ramli, Liyana, Zaharuddin Mohamed, Auwalu M. Abdullahi, Hazriq Izzuan Jaafar, and Izzuddin M. Lazim.: Control strategies for crane systems: A comprehensive review, Mechanical Systems and Signal Processing 95, pp. 1-23, 2017.

- [4] Gu, Xiutao, Yuanqi Li, Mengqing Hong, Song Ye, and Yu Guo.: Fixed time robust control for tower cranes with unmatched disturbances and input saturation, *International Journal of Adaptive Control and Signal Processing* 37, no. 5, pp. 1293-1317, 2023.
- [5] Xia, Jiyu, and Huimin Ouyang: Chattering Free Sliding-Mode Controller Design for Underactuated Tower Cranes With Uncertain Disturbance, *IEEE Transactions on Industrial Electronics* 71, no. 5, pp. 4963-4975, 2023.
- [6] Hou, Chuanjing, Can Liu, Zhi Li, Zheng Xin, and Hanyuan Zhang: Tower crane systems modeling and adaptive robust sliding mode control design under unknown frictions and wind disturbances, *Transactions of the Institute of Measurement and Control*, 2024.
- [7] Yang, Yana, Wenkai Hui, and Junpeng Li: Model-free composite sliding mode adaptive control for 4-DOF tower crane, *Automation in Construction* 167, 2024.
- [8] Hou, Chuanjing, Can Liu, Zhi Li, and Duchun Zhong: An improved non-singular fast terminal sliding mode control scheme for 5-DOF tower cranes with the unknown payload masses, frictions and wind disturbances, *ISA transactions* 149, pp. 81-93, 2024.
- [9] Zhang, Menghua, Xingjian Jing, Zengcheng Zhou, and Weijie Huang: Transportation for 4-DOF Tower Cranes: A Periodic Sliding Mode Control Approach, *IEEE Transactions on Intelligent Transportation Systems*, 2024.
- [10] Chen, He, Yongchun Fang, and Ning Sun. "An adaptive tracking control method with swing suppression for 4-DOF tower crane systems." *Mechanical Systems and Signal Processing* 123, pp. 426-442, 2019.
- [11] Zhang, Menghua, Xingjian Jing, Zengcheng Zhou, and Mingxu Sun: Rapid and restricted swing control via adaptive output feedback for 5-DOF tower crane systems, *Mechanical Systems and Signal Processing* 212, 2024.
- [12] Zhang, Menghua, and Xingjian Jing: Adaptive neural network tracking control for double-pendulum tower crane systems with nonideal inputs, *IEEE Transactions on Systems, Man, and Cybernetics: Systems* 52, no. 4, pp. 2514-2530, 2021.
- [13] Zhang, Menghua, Xingjian Jing, Weijie Huang, Quanli Lu, Jiyang Chen, and Zhenxue Chen: Robust fault accommodation approach for double-pendulum tower cranes via adaptive neural network-triggered control, *Nonlinear Dynamics* 111, no. 21, pp. 19993-20013, 2023.
- [14] Wang, Kai, Xin Ma, and Jing Li: Neural Network-Based Adaptive Swing Suppression Control for Tower Cranes With Obstacle Avoidance, *IEEE/ASME Transactions on Mechatronics*, 2024.
- [15] Zamfirache, Iuliu Alexandru, Radu-Emil Precup, and Emil M. Petriu: Adaptive reinforcement learning-based control using proximal policy optimization and slime mould algorithm with experimental tower crane system validation, *Applied Soft Computing* 160, 2024.
- [16] Mohiuddin, Mohammed Basheer, Igor Boiko, Rana Azzam, and Yahya Zweiri: Closed-loop stability analysis of deep reinforcement learning controlled systems with experimental validation." *IET Control Theory & Applications*, 2024.
- [17] Roman, Raul-Cristian, Radu-Emil Precup, and Emil M. Petriu: Hybrid data-driven fuzzy active disturbance rejection control for tower crane systems, *European Journal of Control* 58, pp. 373-387, 2021.
- [18] Kang, Xinyu, Lin Chai, and Huikang Liu: Anti-swing and Positioning for Double-pendulum Tower Cranes Using Improved Active Disturbance Rejection Controller, *International Journal of Control, Automation and Systems* 21, no. 4, pp. 1210-1221, 2023.
- [19] Al-Fadhli, Abdulaziz, and Emad Khorshid: Payload oscillation control of tower crane using smooth command input, *Journal of Vibration and Control* 29, no. 3-4, pp. 902-915, 2023.
- [20] Alhassan, Ahmad Bala, Wudhichai Assawinchaichote, Huiyan Zhang, and Yan Shi: Hybrid input shaping and fuzzy logic-based position and oscillation control of tower crane system, *Expert Systems* 41, no. 2, 2024.
- [21] Rehman, SM Fasih, et. al.: Input shaping with an adaptive scheme for swing control of an underactuated tower crane under payload hoisting and mass variations, *Mechanical Systems and Signal Processing* 175, 2022.
- [22] Rauscher, Florentin, and Oliver Sawodny: Modeling and control of tower cranes with elastic structure, *IEEE Transactions on Control Systems Technology* 29, no. 1, pp. 64-79, 2020.
- [23] Thomas, Matthias, Tobias Englert, and Oliver Sawodny: Model-based velocity-tracking-control of self-erecting industrial tower cranes, *Control Engineering Practice* 147, 2024.
- [24] J. Chen, J. Wang, Y. Liu, Z. Hu: Design verification of aeroengine rotor speed controller based on U-LADRC, *Math. Problems Eng.*, vol. 2020, pp. 1-12, 2020.
- [25] C. Liu, G. Luo, X. Duan, Z. Chen, Z. Zhang, C. Qiu: Adaptive LADRC-based disturbance rejection method for electromechanical servo system, *IEEE Trans. Ind. Appl.*, vol. 56, no. 1, pp. 876-889, 2020.
- [26] L. Yu, R. Wang, W. Xia, W. Wang: An anti-windup method for a class of uncertain MIMO systems subject to actuator saturation with LADRC, *Inf. Sci.*, vol. 462, pp. 417-429, 2018.
- [27] C. Liu, G. Luo, Z. Chen, W. Tu: Measurement delay compensated LADRC based current controller design for PMSM drives with a simple parameter tuning method, *ISA Trans.*, vol. 101, pp. 482-492, 2020.
- [28] Y. W. Wang et al.: A LADRC-based fuzzy PID approach to contour error control of networked mo-

tion control system with time-varying delays, *Asian J. Control*, vol. 22, no. 5, pp. 1973–1985, 2020.

- [29] C. Li, X. Zhou, Y. Ma, and L. Shao: The LADRC control system of distribution static synchronous compensator based on chaotic sequences PFPWM, *Adv. Sci. Lett.*, vol. 11, no. 1, pp. 556–560, 2012.
- [30] C. Liu, Y. Cheng, D. Liu, G. Cao, and I. Lee: Research on a LADRC strategy for trajectory tracking control of delta high-speed parallel robots, *Math. Problems Eng.*, vol. 2020, pp. 1–12, 2020.
- [31] J. Han: From PID to active disturbance rejection control, *IEEE Trans. Ind. Electron.*, vol. 56, no. 3, pp. 900–906, 2009.
- [32] M. Fliess, et al.: Flatness and defect of non-linear systems: Introductory theory and examples, *Int. J. Control*, vol. 61, no. 6, pp. 1327–1361, 1995.
- [33] H. Li, Y.-B. Hui, Q. Wang, H.-X. Wang, and L.-J. Wang: Design of anti-swing PID controller for bridge crane based on PSO and SA algorithm, *Electronics*, vol. 11, no. 19, p. 3143, 2022.
- [34] Omar, H.M.: Control of gantry and tower cranes, PhD thesis, Virginia Polytechnic Institute and State University, 2003.

КОНТРОЛА ОДБАЦИВАЊА ЛИНЕАРНИХ АКТИВНИХ ПОРЕМЕЋАЈА ЗАСНОВАНА НА РАВНОСТИ ЗА ТОРАЊСКИ КРАН

Т.Л. Тонг, Т.А. Нгујен, М.Д. Донг

Контролисање торањских кранова представља значајне изазове због њихове сложености, нелинеарности и недовољно активираних динамике. Овај рад представља стратегију управљања која интегрише Linear Active Disturbance Rejection Control (LADRC) са теоријом диференцијалне равности да би се постигло прецизно позиционирање колица и ефективно елиминисање замаха. Да бисмо поједноставили системски модел, примењујемо теорију диференцијалне равности да дефинишемо излаз система, омогућавајући нам да третирамо несигурности и спољашње сметње као сингуларни тотални поремећај. Методологија контроле је заснована на принципима LADRC. Поред тога, користимо симулирану оптимизацију роја честица жарења (PSO-SA) за фино подешавање параметара контролера. Резултати симулације показују да предложени метод управљања показује робусне перформансе у односу на 0074 несигурности.